Intramolecular Singlet−Singlet and Triplet−Triplet Energy Transfer in Adamantyl-Linked Trichromophores

Z. Tan, R. Kote, W. N. Samaniego, S. J. Weininger, and W. G. McGimpsey*

Department of Chemistry and Biochemistry, Worcester Polytechnic Institute, Worcester, Massachusetts 01609

Received: May 19, 1999; In Final Form: July 26, 1999

Intramolecular singlet−singlet energy transfer (SSET) has been observed in 4-(3-(*x*-phenanthryl)-1-adamantyl)-4′-(3-(2-naphthyl)-1-adamantyl)biphenyl (**3**), a trichromophoric molecule consisting of phenanthrene, biphenyl, and naphthalene groups linked sequentially by adamantane bridges in which chromophore attachment is at the tertiary 1- and 3-adamantyl positions. UV−visible absorption, steady-state and time-resolved fluorescence, low-temperature phosphorescence and room-temperature laser flash photolysis measurements indicate that efficient SSET takes place with equal probability from the central biphenyl group to each of the terminal chromophores with a rate constant, $k > 6 \times 10^{10}$ s^{-1}. Slower SSET from the naphthyl chromophore to the phenanthryl group occurs with a rate constant $k \sim 9 \times 10^{6}$ s^{-1}. The experimentally determined SSET efficiency and a calculation of the critical Förster distance, when combined with molecular modeling, indicate that a Förster mechanism is sufficient to account for the observed SSET process. Intramolecular triplet−triplet energy transfer (TTET) from the phenanthryl group to the naphthyl chromophore appears to occur by a slow, thermally activated transfer step from the phenanthrene ring to the central biphenyl group followed by rapid exergonic transfer to the naphthyl group. TTET in the reverse direction involving thermal activation of the naphthyl triplet also apparently may take place.

Introduction

Intramolecular charge and energy transfer in bichromophores has been the subject of considerable interest in recent years. Particular attention has been paid to the kinetics of transfer processes and how they are affected by molecular conformation, the rigidity or flexibility of the connecting bridges, and interchromophore distance.[1−37] The observed relationships between the efficiency of transfer and these parameters have been used to investigate the importance of dipole-induced dipole (Förster) and electron exchange (Dexter) transfer mechanisms, as well as the participation of through-bond and through-space transfer routes. For systems that are limited to through-space pathways, it is generally accepted that the dipole-induced dipole mechanism is important at large interchromophore separations while the exchange mechanism predominates at shorter distances. The through-bond superexchange mechanism appears to be favored for molecules in which the chromophores are joined by rigid saturated hydrocarbon bridges such as those synthesized and characterized, for example, by Closs,[1−5] Morrison,[6−12] Paddon-Row and Verhoeven,[13−20] Zimmerman,[21] and others,[22−24] including ourselves.[23] In these bridges, orbital overlap facilitating a super-exchange interaction is provided by an "all-trans" arrangement of the σ bonds. In contrast, bichromophores containing flexible bridges[25−36] allow the chromophore−bridge−chromophore structure to sample many conformations, only a small number of which produce orbital overlap conducive to through-bond transfer. In these molecules, the transfer process has traditionally been regarded as a through-space interaction. (Until recently, the effect of medium on through-space transfer efficiency has been largely ignored, especially in the case of energy transfer.)

Larger molecules containing more than two chromophores have also been studied. Morrison has incorporated singlet and triplet energy donors and acceptors into a steroidal backbone and has observed singlet−singlet and triplet−triplet energy transfer processes occurring with reasonably large rate constants, via a through-bond mechanism.[9−12] Paddon-Row observed rapid charge separation between the terminal chromophores in a trichromophore connected by fused norbornyl spacers.[19] Lindsey has constructed large polychromophores from a series of metalated and free base porphyrin moieties connected by diphenylethyne and *p*-phenylene linkages[37,38] and has observed efficient energy and hole transfer in these molecules. Intramolecular transfer has also been reported in a variety of other trichromophores.[39,40] Some of these studies are founded upon recent literature that suggests large polychromophores could be used as molecular wires and electronic and photonic devices.[41−45] Some of our recently published work also falls into this category. We reported intramolecular energy transfer in the two trichromophoric molecules shown in Scheme 1 (compounds **1** and **2**).[46] In these compounds phenanthrene, biphenyl (or benzophenone), and naphthalene groups are linked sequentially by methyl ester bridges. These molecules essentially act as three distinct chromophores with no discernible ground-state electronic interaction between the moieties. Upon UV excitation, however, both singlet−singlet (SSET) and triplet−triplet (TTET) energy transfer processes are observed. In **1**, rapid ($k > 10^{10}$ s^{-1}) SSET occurs from the central biphenyl group to the phenanthrene and naphthalene chromophores with little discrimination between the two pathways. A slower SSET process from the naphthalene to the phenanthrene group consistent with a longer range interaction and likely involving the Förster mechanism also was observed. In **2**, SSET occurs in the opposite direction—from the terminal chromophores to the benzophenone group—although with a considerably smaller rate constant, which we attributed to a small spectral overlap integral. Following efficient ISC in the benzophenone chromophore, rapid TTET (exchange)

10.1021/jp9916539 CCC: $18.00
Published on Web 09/03/1999

SCHEME 1

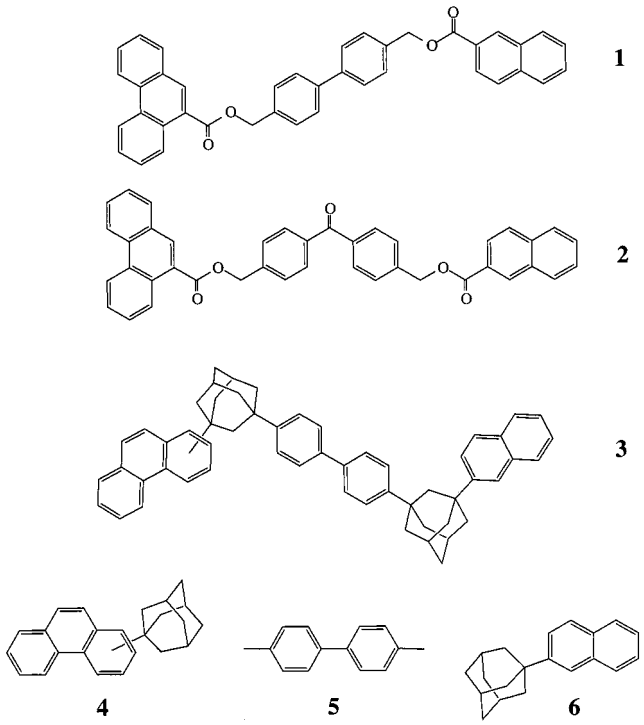

back to the naphthalene and phenanthrene triplet states takes place. TTET between the terminal chromophores was not observed in either **1** or **2**. This behavior is consistent with an interchromophore separation that is sufficiently large (~12 Å) to prevent efficient through-space exchange-type transfer.

We have undertaken the present study for two reasons. First, we have synthesized **3** (shown in Scheme 1 along with the three model compounds that we have used to help characterize its photophysical behavior) in order to further probe transfer processes in trichromophores. In a more general sense, however, we are interested in determining whether polychromophoric molecules such as these could potentially act as molecular scale devices. We have already shown in compound **1** that triplet excitation energy can be optically gated between the naphthyl and phenanthryl terminal chromophores. Essentially, this makes **1** a prototypical optically triggered molecular switch.[46]

The ester bridges in **1** and **2** give the molecules considerable conformational freedom, although in each case the central aromatic chromophore guarantees a minimum separation between the terminal chromophores. Given the possibility of a large number of conformations, it is likely that through-space transfer mechanisms dominate over through-bond pathways in these compounds. Compound **3** differs from **1** and **2** in the nature of the connecting bridges between chromophores; in **3**, the chromophores are linked by 1,3-substituted adamantyl groups. As in polychromophores utilizing cyclohexyl, *trans*-decalin, and steroidal spacers,[1−12] rotational flexibility in this molecule is now limited to the single bonds between chromophore and bridge and the central bond in the biphenyl group. We thus anticipated that through-bond transfer may play a more important role here than in **1** and **2**. In fact, given the quasi-C_3 symmetry at the adamantyl positions (compared to quasi-C_2 in cyclohexanes) we felt that transfer would be more efficient for **3** than for cyclohexane-bridged molecules, since rotation around the chromophore−adamantyl bond would result in a greater number of conformations that are conducive to through-bond transfer.

We present here a study of the energy transfer processes in **3** as characterized by UV−visible, fluorescence and phosphorescence spectroscopies, single photon counting, laser flash photolysis, and molecular modeling methods. Our results indicate that the behavior observed for **3** is similar to that of **1** in that SSET between all three chromophores is observed. However, despite the rigidity of the bridges between chromophores that may be expected (based on the results for other rigid systems described above) to promote efficient transfer, TTET was inefficient.

Experimental Section

Materials and Methods. All solvents and synthetic starting materials were used as received from Aldrich. Solvents used in spectroscopic studies were spectrophotometric grade.

Syntheses: General Methods. Proton nuclear magnetic resonance (^{1}H NMR) spectra were obtained either on a Bruker ACE 200 (200 MHz) NMR spectrometer or a Bruker AVANCE 400 (400 MHz) NMR spectrometer. Chemical shifts are reported in ppm (δ) relative to internal tetramethylsilane (TMS) at 0.00 ppm. Carbon nuclear magnetic resonance spectra (^{13}C NMR) were recorded at either 50 or 100 MHz on the spectrometers mentioned above.

The mass spectrometric evaluations were conducted on a Perceptive Biosystems Voyager DE with a nitrogen laser operating at 337 nm and a 3 ns pulse width. The instrument was operated in the linear mode with an accelerating voltage of 16 kV and a scan delay of 150 ms. Zinc tetraphenylporphyrin in 2,5-dihydroxybenzoic acid was used to provide a two-point external calibration.

The compounds did not produce a molecular ion in either the positive or negative ion modes of operation in the presence of a matrix even when the analytical conditions and concentrations were varied. A short-lived molecular ion was observed if the analyte was exposed directly to the laser without the use of a matrix. Under these conditions the analyte quickly disappeared, but there was sufficient time to average 64 scans per sample.

Analytical thin layer chromatography was performed using precoated silica gel plates (0.25 mm thickness, Merck 60F254) and were visualized under a UV lamp or in a glass chamber containing iodine. Flash chromatography was performed on J. T. Baker 40 μm silica gel under positive pressure of air. Preparative thin layer chromatography was performed using precoated silica gel plates (1000 μm thickness, Merck 60F254). Melting points were determined on a Thomas-Hoover capillary melting point apparatus and are uncorrected.

All reactions were carried out under nitrogen unless otherwise stated. All extracts were dried over $MgSO_4$ unless otherwise stated.

Descriptions of the syntheses are provided in the Supporting Information.

Absorption and Emission Spectroscopy. Ground-state absorption spectra and extinction coefficients were obtained with a Shimadzu 2100U absorption spectrometer. Fluorescence emission spectra and quantum yields were measured in nitrogen- and air-saturated cyclohexane and were found to be independent of saturating gas. Spectra were recorded with a Perkin-Elmer LS-50 spectrofluorometer. Yields were measured using the parent aromatic molecules as standards.[12] Phosphorescence spectra were recorded with the same instrument. Samples were in 1:1 ethanol:methanol glasses at 77 K.

Laser Flash Photolysis. The laser flash photolysis system has been described in detail elsewhere.[47] Briefly, for kinetic studies and transient absorption spectra, solutions were prepared

TABLE 1: Ground-State Extinction Coefficients and Initial Excitation Distributions (ED Values) for Compounds 3−6

	3 (trichromophore)	**4** (phenanthryladamantane)	**5** (dimethylbiphenyl)	**6** (naphthyladamantane)
ϵ_{226}[a]	103 000	12 700	3100	104 000
ϵ_{256}	74 600	53 400	15 200	3900
ϵ_{303}	1680	100	30	400
ED_{226}, %		11	2	87
ED_{256}, %		74	21	5
ED_{303}, %		70	2	28

[a] Extinction coefficients have an estimated error of ± 5.0%

TABLE 2: Fluorescence Maxima, Quantum Yields, Singlet Energies and Lifetimes, and Triplet Energies for 3−6

	3 (trichromophore)	**4** (phenanthryladamantane)	**5** (dimethylbiphenyl)	**6** (naphthyladamantane)
λ_{max}	333 (major peak)	350 (peak)	314 (shoulder)	327 (peak)
(λ_{ex} = 226 nm)	349 (major peak)	359 (shoulder)	322 (major peak)	334 (major peak)
	365 (peak)	368 (major peak)	334 (shoulder)	
	384 (shoulder)	384 (peak)		
Φ_{Fl}[a]		0.13	0.32	0.37
τ_s (ns)	2.4 (0.8)	2.5 (0.8)	14.9	66
	45 (0.2)	49 (0.2)	(λ_{ex} = 290 nm)	(λ_{ex} = 313 nm)
	(λ_{ex} = 313 nm)	(λ_{ex} = 313 nm)		
E_s[b] (kcal/mol)		84.9	96.6	91.4
E_t[c] (kcal/mol)		62.1	64.2	61.6

[a] Independent of wavelength. [b] From fluorescence and absorption data. [c] From phosphorescence data. Wavelengths quoted are ±1 nm.

at concentrations sufficiently large to give absorbances in the range 0.6−0.8 at the excitation wavelength. Unless otherwise noted, the solutions, contained in a reservoir, were continuously purged with a stream of nitrogen and were caused to flow through a specially constructed quartz cell (7 mm × 7 mm) by means of a peristaltic pump. This ensured that a fresh volume of solution was exposed to each laser pulse, thereby avoiding accumulation of any photoproducts. Samples were irradiated with the pulses of a Lumonics EX 510 excimer laser (308 nm; ∼20 mJ/pulse; 8 ns pulse duration) or the frequency-tripled output of a Continuum Nd:YAG laser (355 nm, ∼30 mJ/pulse, 5 ns).

Calculations. To obtain minimum energy conformations of the trichromophores, conformational space was explored using ChemPlus 1.5 and the MM+ force field. The lowest energy conformations were further minimized using AM1 and PM3 parameters in the Hyperchem semiempirical option. These minimized conformations were used to obtain the spectroscopic energies with ZINDO/S parameters. Calculations were carried out on a 200 MHz Pentium PC.

Results and Discussion

(i) Absorption and Fluorescence Measurements. Table 1 gives ground-state extinction coefficients for **3** and its model compounds **4**−**6** at various wavelengths in the UV. These spectra as well as the results of AM1 and ZINDO/S calculations indicate that the ground state of **3** behaves spectroscopically and electronically as the sum of three isolated chromophores. The absorption spectrum for **3** is similar in band shape and extinction coefficient to a composite spectrum that was constructed by adding proportional contributions from the model compounds, suggesting that there is little interaction in the ground state between the chromophores. AM1 and ZINDO/S calculations indicate that the highest energy occupied molecular orbitals (highest 6) and the lowest energy unoccupied molecular orbitals (lowest 6) are likely localized on individual chromophores. In addition, the *relative* energies predicted by ZINDO/S for the HOMO−LUMO transitions in **3** are consistent with experimental absorption spectra of the model compounds. Therefore, it is likely that excitation of the localized ground state of one of the chromophores initially will result in the production of an excited state that is also localized on the same chromophore. As a result, the extinction coefficients of the model compounds at each wavelength can be used to estimate how the initial excitation is partitioned among the chromophores in **3**. These initial excitation distributions (ED), expressed as percentages for each excitation wavelength are also shown in Table 1. For example, we estimate that exposure of **3** to λ_{ex} = 226 nm results in the following ED values: phenanthryl, 11%; biphenyl, 2%; naphthyl, 87%. As is indicated by the ED values in Table 1, the wavelengths chosen correspond to quite different absorption conditions. These wavelengths—226, 256, and 303 nm—were chosen to provide the maximum possible excitation of the naphthalene, biphenyl, and phenanthrene chromophores, respectively. Thus, at 226 nm most of the incident light is absorbed by the naphthalene chromophore while at 256 nm the phenanthrene and biphenyl chromophores absorb more strongly than naphthalene (at no wavelength was the biphenyl chromophore the major absorber). At 303 nm most of the excitation takes place in the phenanthrene chromophore with a lesser amount of absorption in the naphthalene group. The effect of using these different excitation wavelengths is reflected in the fluorescence and phosphorescence emission measurements.

Table 2 shows the fluorescence maxima, quantum yields, singlet energies, and lifetimes measured for **3** and its model compounds. (We note that the fluorescence decay of the phenanthryladamantane model exhibits a double exponential that may be due to the presence of both 2- and 3-substituted isomers.) Figure 1 shows the emission spectrum (λ_{ex} = 256) of **3** as well as the spectra of its associated model compounds. Spectra for the model compounds were identical at the other excitation wavelengths, while the spectra of **3** showed minor, but significant, wavelength effects that are discussed later. It is immediately apparent from these spectra that the emission of **3** consists of contributions from both phenanthrene and naphthalene groups. Illustrating this behavior, Figure 2 shows the emission spectrum of **3** (λ_{ex} = 256 nm) along with a composite spectrum (composite spectrum A) constructed by summing the emission spectra of all three chromophores in the proportion indicated by their initial ED values for this wavelength (i.e., 0.74 (**4**) + 0.21 (**5**) + 0.05 (**6**)). The most striking feature of the measured spectrum of **3** when compared to the composite

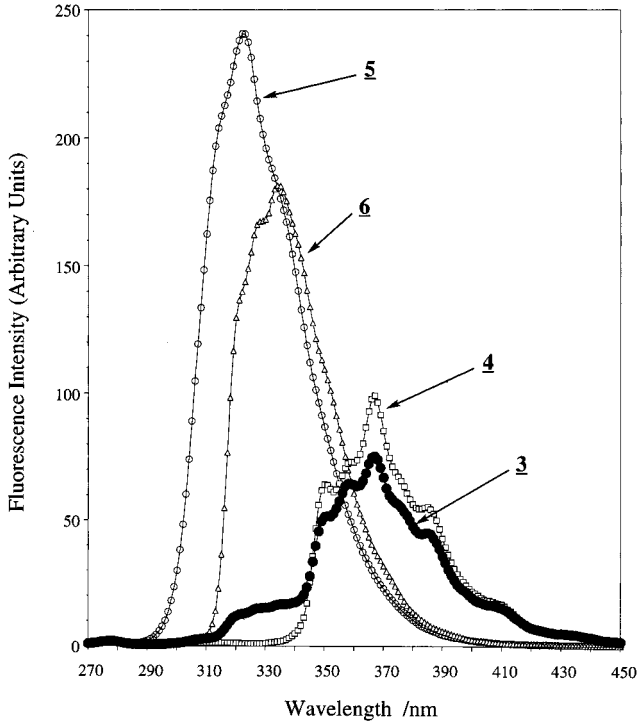

Figure 1. Fluorescence emission spectra of **3** and its model compounds **4**−**6** in nitrogen-saturated cyclohexane, λ_{ex} 256 nm. All samples had identical absorbance at the excitation wavelength.

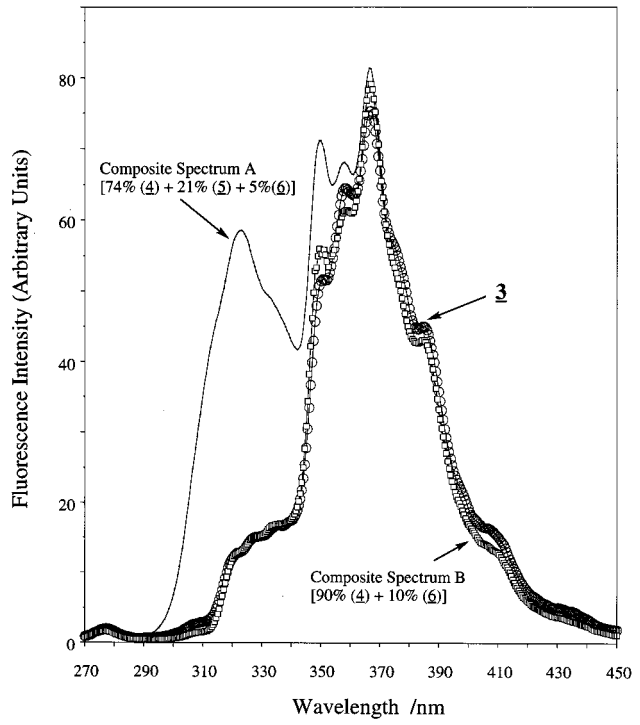

Figure 2. Fluorescence emission spectrum of **3** in nitrogen saturated cyclohexane (round symbols). Also shown are composite spectra constructed (i) by assuming that all three chromophores emit according to the initial excitation distributions (composite spectrum A) and (ii) by assuming only phenanthryl and naphthyl chromophores emit (composite spectrum B). The 90:10 ratio represents a best fit to the spectrum of **3**.

spectrum is the absence of any evidence for emission from the biphenyl moiety. While it could be argued that the relatively small absorption expected for the biphenyl chromophore at λ_{ex} = 226 and 303 nm is responsible for the lack of biphenyl emission, the spectrum shown was obtained at λ_{ex} = 256 nm,

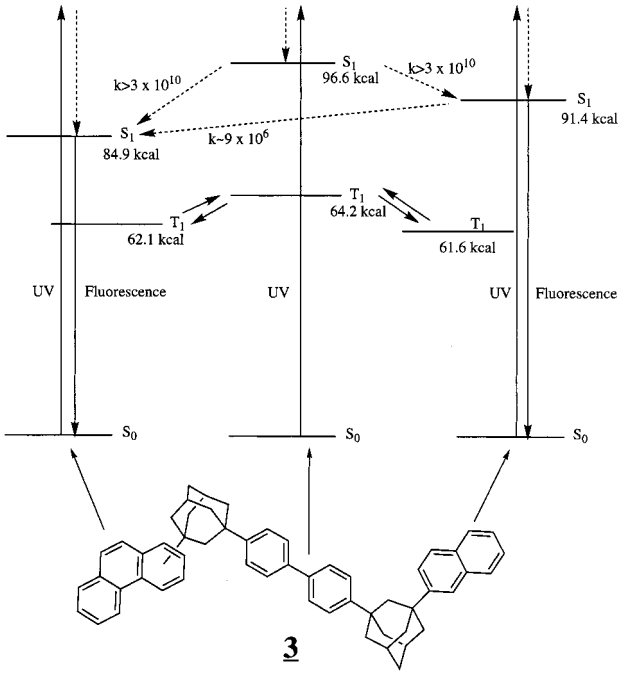

Figure 3. Energy diagram showing the intramolecular SSET and TTET processes and estimated rate constants.

where 21% of the absorption is due to the biphenyl group. No biphenyl emission was observed.

It is clear from the emission spectra of **3** obtained at all excitation wavelengths that the contribution due to naphthalene is considerably different from that expected from the ED for this chromophore. To determine the actual contribution of the naphthalene chromophore to the emission spectrum of **3**, composite spectra were created in which no biphenyl emission was included and in which the relative contributions of naphthalene and phenanthrene were varied. Figure 2 also shows a composite spectrum (composite spectrum B) constructed by assuming a 90:10 ratio of emission intensities, i.e., 0.90 (**4**) + 0.10 (**6**). This particular ratio accurately reproduces the spectrum of **3**. Small changes in this ratio (more than ±∼1% change in the distribution of each chromophore) result in distinct changes in spectral shape of the composite spectrum, and for this reason we are confident that the ratio used is an accurate reflection of the relative contributions of the phenanthrene and naphthalene chromophores. This method was also used successfully to reproduce the spectra of **3** obtained at λ_{ex} = 226 and 303 nm. For these latter wavelengths, the **4**:**6** ratios for the matching composite spectra were 40:60 and 83:17, respectively.

(ii) Singlet−**Singlet Energy Transfer (SSET).** The results described above for **3** are consistent with the energy transfer mechanism shown in Figure 3. The results support three intramolecular SSET pathways: biphenyl → phenanthrene, biphenyl → naphthalene, and naphthalene → phenanthrene. From the singlet energies given in Table 2, it is clear that energy transfer from the biphenyl singlet to both the phenanthrene and naphthalene chromophores is energetically possible, as is further energy transfer from naphthalene to phenanthrene. That energy transfer occurs rapidly from the biphenyl chromophore is most distinctly illustrated by the lack of observed biphenyl emission, even at λ_{ex} = 256 nm, where the biphenyl absorption is substantial. Since product studies carried out under CW lamp irradiation of **3** failed to show any significant conversion of starting material, an efficient chemical deactivation pathway for singlet excited **3** is unlikely. Also, while intermolecular processes, including energy transfer, could account for singlet

TABLE 3: Initial, Intermediate, and Final Excitation Distributions (4:5:6)

excitation wavelength	initial excitation distribution (ED)	intermediate excitation distribution[a]	final distribution
226 nm	11:2:87	12:0:88	40:0:60
256 nm	74:21:5	84.5:0:15.5	90:0:10
303 nm	71:2:27	72:0:28	83:0:17

[a] Assuming equal partition of biphenyl singlet excited states.

quenching given sufficiently high concentrations of **3**, the maximum concentration of **3** used in any of the fluorescence experiments was less than 80 μM. This low concentration, coupled with the short singlet lifetime for **5**, $\tau = 14.9$ ns, suggests that diffusion-controlled intermolecular quenching ($k \sim 10^{10}$ $M^{-1}s^{-1}$) is not significant. It is thus likely that the deactivation of the biphenyl singlet is due to intramolecular SSET. One assumption made in reaching this conclusion is that the efficiency of *intra*chromophore deactivation processes in **5** is not significantly altered when the chromophore is incorporated into **3**. While it is not possible to determine with complete certainty the effect of the neighboring chromophores on such processes as internal conversion and ISC, the lack of interaction between chromophores in the ground state argues against a large effect.

Evidence for energy transfer from the naphthalene moiety to the phenanthrene group can be found in the spectra generated at all three excitation wavelengths and by a comparison of these spectra with the composite spectra. The spectra at $\lambda_{ex} = 226$ and 303 nm provide the most direct indication of naphthalene−phenanthrene energy transfer. Clearly, the ratio of naphthalene to phenanthrene emission as indicated from the composite spectrum is considerably smaller than that expected from the initial ED. This indicates that some of the naphthalene singlet states initially produced are subsequently quenched. Since energy transfer to biphenyl is uphill energetically and there was no observed chemical conversion, this quenching must be due to either *inter*- or *intra*molecular energy transfer to the phenanthrene group. The measured singlet lifetime of the naphthalene model compound, **6**, is 66 ns. Therefore, the same argument used against *inter*molecular energy transfer for the biphenyl moiety can also be used here. That at least some of the naphthalene emission was not quenched while that of biphenyl was completely quenched is consistent with the larger interchromophore distance for naphthalene−phenanthrene and the attendant smaller rate constant expected for energy transfer (vide infra).

The results obtained at 256 nm were somewhat different from those at the other two excitation wavelengths but can still be explained in the context of naphthalene−phenanthrene energy transfer. The absorption due to the naphthalene group in **3** at 256 nm is minor (5%) compared to that of phenanthrene and biphenyl. The composite spectrum that most closely reproduced the actual emission spectrum (Figure 2) indicates a 10% contribution due to naphthalene, i.e., an increase over the initial ED rather than a decrease, as observed at 226 and 303 nm. This result would appear to be at odds with the energy transfer interpretation described above. However, if decay of the biphenyl singlet state partitions between naphthalene and phenanthrene and if the rate of transfer is rapid compared with subsequent naphthalene−phenanthrene SSET, the actual concentration of naphthalene singlet states produced following 256 nm excitation will be considerably greater than 5%. Table 3 shows the initial ED, the distribution of excited states assuming equal partitioning of the biphenyl excitation to phenanthrene and naphthalene, and the final excitation distribution as determined from emission data (from composite spectra). In this scenario, then, the reduction in the naphthalene distribution from its value following biphenyl energy transfer to that indicated by the emission spectra reflects the actual efficiency of energy transfer quenching of the naphthalene singlet state.

While it is not possible to determine directly whether the biphenyl singlet energy partitions equally between the naphthalene and phenanthrene chromophores, the results in Table 3 suggest that an equal division does occur. The ratio of naphthalene fluorescence assuming equal partitioning (column 2 in Table 3) to the actual naphthalene emission (column 3) is virtually the same at all three wavelengths, i.e., under conditions where the biphenyl chromophore is excited to a substantial extent (20% at 256 nm), and under conditions where there is very little direct biphenyl excitation. This means that excitation of the biphenyl chromophore does not change the final distribution of excited states in favor of one chromophore over the other. This effect could only occur if energy transfer from biphenyl does not differentially bias the population of the phenanthrene and naphthalene singlet states. Computer modeling of the structure of **3** (vide infra) supports this suggestion.

These fluorescence emission data contain information on the rates of biphenyl−naphthalene−phenanthrene SSET. In the case of energy transfer from biphenyl, the lack of any observable biphenyl emission is an indication that transfer is quite rapid. The sensitivity of our fluorometer is such that we are able to observe emission intensities as low as 0.1% of the level that was recorded for **5**. Given that the rate constant for deactivation of singlet **5** (obtained from fluorescence lifetime measurements) is $k_s = 6.25 \times 10^7$ s^{-1}, we infer that the lower limit for the SSET quenching rate constant is 6×10^{10} s^{-1}. Since SSET to each of phenanthrene and naphthalene appears to occur with equal efficiency, the lower limit for the rate constants of the individual SSET pathways is 3×10^{10} s^{-1}.

The extent to which the naphthalene emission is attenuated in **3** allows an estimate of the naphthalene−phenanthrene energy transfer rate constant. This attenuation can be calculated by comparing the intermediate ED value for the naphthyl chromophore in **3** with the final ED value as determined from the composite spectra. The intermediate ED represents the extent of naphthyl emission in the absence of a singlet energy acceptor. The final ED represents the actual naphthyl emission and is smaller than ED(intermediate) due to SSET to the phenanthryl group. The ratio of the two values (ED(final)/ED(intermediate)) is equivalent to the ratio of fluorescence quantum yields in the absence and in the presence of the acceptor and is equal to the emission efficiency. The ED data in Table 3 indicate that as an average over the three excitation wavelengths, the emission efficiency for the naphthyl chromophore in **3** is 0.63 ± 0.05. Using this value in eq 1 yields an estimate of the energy transfer rate constant, k_{SSET}. In eq 1, k_F is the radiative rate constant for

$$\frac{\Phi_3^F}{\Phi_6^F} = \frac{ED_{Final}}{ED_{Intermediate}} = \frac{k_F/(k_{all} + k_{ET})}{k_F/k_{all}} = \frac{k_{all}}{k_{all} + k_{ET}} \qquad (1)$$

the naphthyl chromophore and is assumed to be equal in both **3** and **6** and k_{All} is the sum of the rate constants for all intrachromophore deactivation processes including k_F, k_{IC}, and k_{ISC} and is equivalent to the rate constant obtained from the fluorescence lifetime measurements. Using this equation yields $k_{SSET} = 9 \times 10^6$ s^{-1}, which is more than 3 orders of magnitude less than the estimated biphenyl−phenanthrene (or naphthalene) energy transfer rate constant (vide infra).

(iii) Triplet−Triplet Energy Transfer (TTET). Phosphorescence spectra of **3** and its model compounds measured in 77

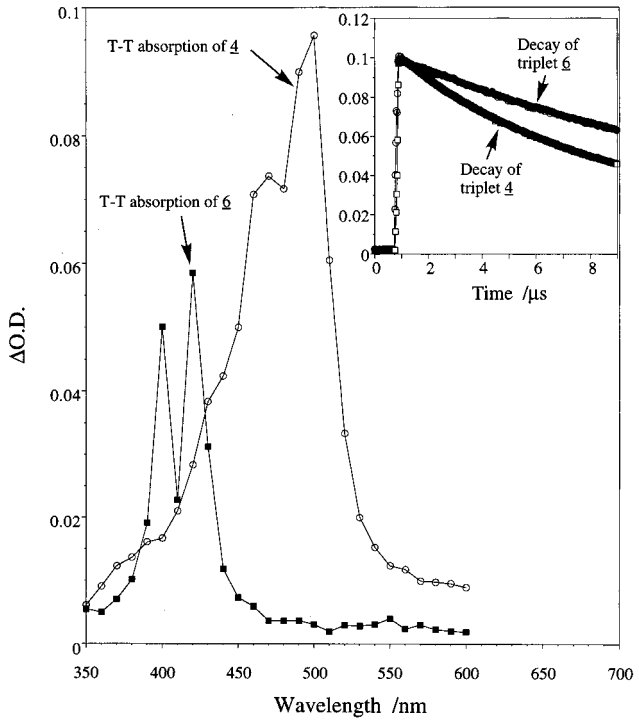

Figure 4. Triplet−triplet absorption spectra obtained 1 μs following 308 nm laser photolysis of **4** and **6** in nitrogen-saturated cyclohexane. Inset: Decay of T−T absorptions of **4** (at 490 nm) and **6** (at 420 nm) obtained under the same conditions as above.

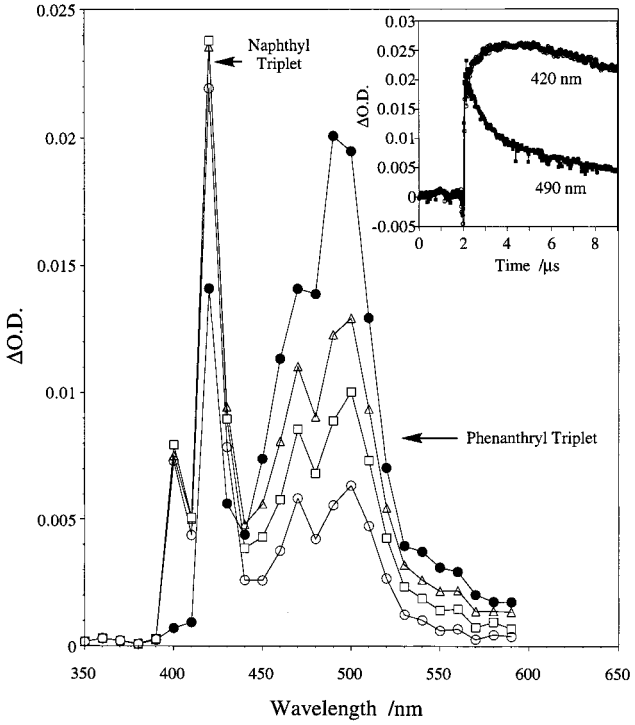

Figure 5. Transient absorption spectra obtained at 4 delay times after 308 nm laser photolysis of **3** in nitrogen-saturated cyclohexane: filled circles, 0.4 μs; triangles, 1.5 μs; squares, 2.5 μs; open circles, 4.5 μs. Inset: Transient decay kinetics obtained at 490 nm (phenanthryl triplet) and 420 nm (naphthyl triplet) under the same conditions as above.

K methylcyclohexane glasses yield the triplet energies shown in Table 2. The band shapes for the model compounds **4** and **6** were similar, indicating similar triplet energies for the two chromophores, in agreement with literature spectra for the parent aromatics.[48] The spectra of **4** and **6** were substantially different in that the phenanthryladamantane exhibited a much more intense spectrum. The spectral band shape of **3** was similar to both **4** and **6** with an intensity intermediate between that of the two models. Also, the intensity of **3** changed with excitation wavelength, mirroring the changes in ED. TTET between the two terminal chromophores could result in either complete or partial quenching of the phenanthryl triplet (since it lies higher in energy) or in an equilibrium between the two triplets due to the relatively small energy difference, as has been reported previously.[49] Given the wavelength dependence of the emission intensity, an equilibrium is unlikely. Also, since at wavelengths where the ED strongly favors the phenanthryl chromophore the emission is very similar to that of **4**; energy transfer from the phenanthryl group to the naphthyl chromophore is unlikely.

Absent from the phosphorescence spectrum of **3** was emission from the biphenyl group, even when excitation wavelengths with a substantial biphenyl ED were used. Although this would seem to indicate efficient TTET from biphenyl to the other groups, it is likely that triplet biphenyl is not populated to any great extent. As already noted, SSET from biphenyl occurs very rapidly and is approximately 3 orders of magnitude faster than the rate reported for S → T ISC in **5**.

Laser flash photolysis (308 nm) of **3** and its models results in the transient absorption spectra and transient kinetics shown in Figures 4 and 5. From the observed effect of oxygen, which caused a dramatic decrease in the transient lifetimes, and from the published transient spectra of the parent aromatic compounds,[50] the absorptions produced by irradiation of the models **4** and **6** (Figure 4, inset shows kinetic decays) can be attributed to the triplet states. (The spectrum of **5** is not shown since the ground-state absorption of this chromophore is negligible at the laser excitation wavelength.) Clearly, the spectrum of **3** (Figure 5—small differences between the model spectra in Figure 4 and the spectrum in Figure 5 at wavelengths less than 400 nm are due to poorly corrected fluorescence) includes contributions from the absorptions of both the phenanthryl and naphthyl triplets. The transient kinetics shown in Figure 5 (inset) suggest the routes for production and decay of these species. The growth of the phenanthryl triplet in **3** occurs within the duration of the laser pulse, likely as a result of direct population via ISC from the phenanthryl singlet state. The production of the naphthyl triplet in **3** has two components, an "instantaneous" growth and a resolved growth. The former is also likely due to direct population via the singlet state since both the naphthyl and phenanthryl chromophores have significant absorption at the laser wavelength. The slower, resolved growth suggests that a TTET sensitization process occurs. Support for identifying TTET as this sensitization process comes from the decreased lifetime of the phenanthryl triplet in **3** as compared with the lifetime for triplet **4**, as well as a rough correlation between the kinetics of the initial component of the phenanthryl triplet decay and the resolved growth of the naphthyl triplet. Since the observed growth rate is independent of the concentration over an order of magnitude concentration change, the sensitization process is unlikely to be intermolecular in origin. However, modeling studies (discussed below) suggest a large interchromophore separation and therefore it is not likely that direct intramolecular TTET from the phenanthryl to naphthyl triplet state is efficient. An alternative explanation could be that phenanthryl → naphthyl TTET occurs via the biphenyl chromophore. The biphenyl triplet state lies only 2.1 kcal/mol higher than the phenanthryl triplet and therefore should be accessible from the phenanthryl triplet following thermal activation. (This behavior was not possible in compound **1** because the carbonyl functionality attached to the phenanthryl and naphthyl chro-

mophores in **1** lowers their triplet energies by several kcal/mol.)[46] Supporting this suggestion is the observation that the phenanthryl triplet decay becomes more rapid at elevated temperatures. Thus, when the temperature is increased from 25 to 50 °C the decay rate constant increases by a factor of ~3. An approximate calculation from these observations yields an activation energy of ~4 kcal/mol, double the difference in triplet energies. However, given that energy transfer to triplet biphenyl is expected to involve a considerable entropic effect due to the conformational changes in biphenyl that occur upon excitation,[49] this is not an unreasonable value.

Thus, in this scenario we suggest that naphthyl triplet formation occurs via activated TTET from phenanthryl to biphenyl chromophores followed by a rapid exergonic transfer from biphenyl to naphthyl. The resolved naphthyl triplet growth and phenanthryl triplet decay reflect the kinetics of the activation step. We encountered two complicating factors in seeking to confirm this behavior. First, the fluorescence of the phenanthryl chromophore occurs at the same wavelength as the biphenyl T−T absorption, making observation of the latter problematic. Second, the naphthyl triplet lies within 2.6 kcal/mol of the biphenyl triplet state and therefore also could undergo activated TTET to the biphenyl triplet. The fact that the temperature dependence of the phenanthryl triplet decay did not exhibit Arrhenius behavior indirectly supports this suggestion. We are currently investigating this effect in greater detail. Figure 3 summarizes these preliminary interpretations.

(iv) SSET and TTET Mechanisms. Correlation with Molecular Structure. SSET is normally discussed in terms of Förster (dipole-induced dipole or radiative) and/or Dexter (electron exchange) mechanisms.[51] When the energy transfer process is intramolecular, superexchange involving through-bond transfer may also be operative. This latter process is usually most effective when the saturated hydrocarbon structure linking the chromophores is rigid and the bonds in the linker are all trans.[1−21,23] We therefore expectated that **3** would be more effective in promoting through-bond superexchange than the flexibly linked compounds **1** and **2** and that a faster SSET rate could potentially be observed. It was anticipated that this factor would have the greatest influence on the interaction between the central and terminal chromophores. However, our study of **1** showed that even when the chromophores are flexibly linked, SSET between these groups is faster than the resolution of our instrumentation. Thus, a direct comparison of rigidly linked **3** with flexibly linked **1** is limited to SSET between the terminal chromophores. As we outline below, Förster theory is sufficient to describe SSET between naphthyl and phenanthryl groups in **3**.

The importance of intramolecular Förster transfer can be determined by the following procedure. The energy transfer efficiency E_{SSET} is calculated from eq 2, where E_F, the

$$E_{SSET} = 1 - E_F \qquad (2)$$

fluorescence efficiency was determined from eq 1. According to Förster theory, E_{SSET} is given by eq 3 where R_0 is the critical Förster separation, the distance at which the rates of energy

$$E_{SSET} = \frac{1}{1 + \frac{R^6}{R_0^6}} \qquad (3)$$

transfer and the intrinsic deactivation of the donor excited state in the absence of the acceptor are the same, i.e., 50% transfer efficiency, and R is the actual interchromophore separation.[51] In turn, R_0 is calculated from eq 4. The value of R determined

$$R_0^6 = \frac{9000 \ln(10) \kappa^2 \Phi_D}{128 n^4 \pi^5 N_A} \int_0^\infty f_D(\nu) e_A(\nu) \nu^{-4} \, d\nu \qquad (4)$$

in eq 3 can then be compared with that obtained by an estimate of the interchromophore distance from the known structure and/or by molecular modeling. Agreement between these R values usually indicates that Förster transfer is the dominant transfer mechanism. In eq 4, Φ_D is the fluorescence quantum yield of the donor in the absence of acceptor, n is the refractive index of the solvent, N_A is Avogadro's number, κ^2 is a term that describes the relative orientation of the transition dipoles for the donor and acceptror groups (usually assigned a value of $^2/_3$ in the case of freely rotating chromophores) and the spectral overlap integral is calculated from $f_D(\nu)$, the emission spectrum (the integral is normalized to 1), and ϵ_A, the molar absorption spectrum.

TABLE 4: Förster Energy Transfer Parameters[a]

chromophore interaction	efficiency		R_0 (eq 4)		R_{calc} (eq 3)		R (modeling)	
	3	1	3	1	3	1	3	1
biphenyl−phenanthryl	~1.0	~1.0	15.6	21.7	*b*		6.1	4.5
biphenyl−naphthyl	~1.0	~1.0	13.5	18.3	*b*		6.0	4.3
phenanthryl−naphthyl	0.37	~0.85	14.3	17.3	15.7	12.3	14.3	11.5

[a] All separations given in Å. [b] See text.

Table 4 provides the experimentally derived transfer efficiency for **3** (eq 2), as well as the values of R_0 calculated from the spectral data of the model compounds **4**−**6**. For comparison, included in the table are values calculated for compound **1**. Combining the efficiency and critical separation values yields an interchromophore separation that should be close to the actual separation if Förster transfer is the dominant transfer mechanism. These calculated separation distances are also given in the table as R_{calc}.

We have also modeled the structure of **3** so as to obtain interchromophore separations.[52] Conformational space was studied using Hyperchem 5.0 and Chemplus. Charges for the initial conformation were obtained using the AM1 model. The MM+ force field was then used to assess the total energy while the variations of the five torsional angles that correspond to the "freely" rotating bonds between the adamantyl bridges and the chromophores was followed. This procedure yielded 12 low-energy conformations, separated by a maximum of 1.5 kcal. Individual rotational barriers around these bonds were calculated, yielding a range from a minimum of 0.93 kcal/mol (phenyl−phenyl bond), to 1.16 kcal/mol (adamantyl−phenanthrene bond). Although the use of molecular mechanics in this case (no heteroatoms) could be considered a good approximation, the 12 conformations were also studied using the AM1 and MNDO semiempirical models. The results were somewhat different, although in both methods the minimum energy conformation was the same as that determined through the MM+ force field. The maximum separation in this case was ca. 0.5 kcal/mol for the different conformers, and the rotational barriers ranged from 1.22 kcal/mol (adamantane−naphthalene bond) to 1.85 kcal/mol (phenyl−phenyl bond). The minimum distance between naphthalene and phenanthrene chromophores for the lowest energy conformation was 16.0 Å. Over all of the low-energy conformations the minimum naphthyl−phenanthryl separation ranged between 12.28 Å (MM+)/12.21 Å (AM1) and 16.24 Å (MM+)/16.05 Å (AM1).

The conformational picture that emerges from these calculations, then, is one in which several low-energy conformations likely contribute to an average structure (the calculated rotational barriers are sufficiently small so as not to impede interconversion at ambient temperatures). Interchromophore separations for **3** shown in Table 4 are averages over all of the low-energy conformations investigated (e.g., the calculated phenanthryl−naphthyl separation was 14.3 Å). These averages do not take into account preferences for one conformation over another since weighting conformations according to the minimum energies calculated would likely represent an overinterpretation of the results. Nevertheless, given that the lowest energy conformation had an interchromopore separation significantly larger than the calculated average and that, generally, conformations with larger separations had lower energies, it is reasonable to suggest that the most probable separation is greater than 14.3 Å.

The naphthyl−phenanthryl separation determined by modeling is the same as the critical Förster distance and suggests that the transfer efficiency should be 50%. Alternatively, the experimental efficiency points to an interchromophore separation of 15.7 Å if SSET proceeds by Förster transfer. Given the approximations made in the calculation of R_0 (e.g., κ, and the overlap integral) and the range of separations obtained from the modeling studies, as well as the indication that the lower energy conformations had larger separations, we conclude that there is little significant difference between these two values and that Förster theory is adequate to describe SSET in **3**. Support for this conclusion is given by the similar observations obtained for **1**, in which the flexible bridges likely limit SSET to the Förster mechanism. The lack of superexchange transfer in **3** despite the rigid adamantyl linkers is ascribed to the remaining conformational flexibility in the molecule, the large number of bonds separating the terminal chromophores, and the unknown effect of the central biphenyl chromophore on the efficiency of superexchange-type transfer.

As mentioned above, the relatively short distance between central and terminal chromophores results in very rapid SSET such that it is not possible to determine the relative contributions to SSET due to Förster, through-space exchange (Dexter), and superexchange mechanisms. It is generally accepted that, at short distances, the Dexter mechanism dominates, and we speculate that a combination of through-space exchange and superexchange may contribute to SSET in this case. We are currently carrying out studies to investigate the contributions of these processes in adamantyl-linked bichromophores.

TTET is almost exclusively an exchange process since the triplet−singlet interaction usually suffers from poor spectral overlap. Exchange transfer requires close approach of the donor and acceptor (essentially a collision) in order to have high efficiency and, for interchromophore separations greater than ~10 Å, is usually not considered efficient. For this reason, direct, through-space phenanthryl → naphthyl TTET in **3**, where the interchromophore separation is about 15 Å, is unlikely. This gives indirect support for the participation of the biphenyl triplet in the observed phenanthryl−naphthyl TTET by the activated process proposed above, but the role of through-bond superexchange TTET could not be determined with certainty in the present study.

Acknowledgment. The authors acknowledge the financial support of the National Science Foundation (CHE-9671830). We also thank the donors of the Petroleum Research Fund administered by the American Chemical Society for partial support of this work. Fluorescence lifetime facilities were made available by Dr. Linda Johnston (National Research Council Canada) and Dr. Robert Redmond (Wellman Laboratories of Photomedicine). High Resolution MS was provided by Dr. Joel Carlson (U.S. Army Soldier Systems Center, Natick Massachusetts). We are also grateful to Professor Pierre Laszlo for helpful discussions.

Supporting Information Available: Synthetic details for all compounds are available. This information is available free of charge via the Internet at http://pubs.acs.org.

References and Notes

(1) Closs, G. L.; Johnson, M. D.; Miller, J. R.; Piotrowiak, P. *J. Am. Chem. Soc.* **1989**, *111*, 3751.
(2) Sigman, M. E.; Closs, G. L. *J. Phys. Chem.* **1991**, *95*, 5012.
(3) Closs, G. L.; Calcaterra, L. T.; Green, N. J.; Penfield, K. W.; Miller, J. R. *J. Phys. Chem.* **1986** *90*, 3673.
(4) Johnson, M. D.; Miller, J. R.; Green, N. S.; Closs, G. L. *J. Phys. Chem.* **1989**, *93*, 1173.
(5) Chattoraj, M.; Bal, B.; Closs, G. L.; Levy, D. H. *J. Phys. Chem.* **1991**, *95*, 9666.
(6) Morrison, H.; Pallmer, M.; Loeschen, R.; Pandey, B.; Muthuramu, K.; Maxwell, B. *J. Org. Chem.* **1986**, *51*, 4676.
(7) Morrison, H. *Rev. Chem. Intermed.* **1987**, *8*, 125.
(8) Wu, Z.-Z.; Morrison, H. *Photochem. Photobiol.* **1989**, *50*, 525.
(9) Wu, Z.-Z.; Morrison, H. *J. Am. Chem. Soc.* **1992**, *114*, 4119.
(10) Wu, Z.-Z.; Nash, J.; Morrison, H. *J. Am. Chem. Soc.* **1992**, *114*, 6640.
(11) Agyin, J. K.; Morrison, H.; Siemiarczuk, A. *J. Am. Chem. Soc.* **1995**, *117*, 3875.
(12) Agyin, J. K.; Timberlake, L. D.; Morrison, H. *J. Am. Chem. Soc.* **1997**, *119*, 7945.
(13) Oevering, H.; Paddon-Row, M. N.; Heppener, M.; Oliver, A. M.; Cotsaris, E.; Verhoeven, J. W.; Hush, N. S. *J. Am. Chem. Soc.* **1987**, *109*, 3258.
(14) Oliver, A. M.; Craig, D. C.; Paddon-Row, M. N.; Kroon, J.; Verhoeven, J. W. *Chem. Phys. Lett.* **1988**, *150*, 366.
(15) Clayton, A. H. A.; Ghiggino, K. P.; Wilson, G. J.; Keyte, P. J.; Paddon-Row, M. N. *Chem. Phys. Lett.* **1992**, *195*, 249.
(16) Kroon, J.; Oevering, H.; Verhoeven, J. W.; Warman, J. M.; Oliver, A. M.; Paddon-Row, M. N. *J. Phys. Chem.* **1993**, *97*, 5065.
(17) Lawson, J. M.; Paddon-Row, M. N.; Schuddeboom, W.; Warman. J. M.; Clayton, A. H. A.; Ghiggino, K. P. *J. Phys. Chem.* **1993**, *97*, 13099.
(18) Paddon-Row, M. N. *Acc. Chem. Res.* **1994**, *27*, 18.
(19) Roest, M. R.; Lawson, J. M.; Paddon-Row, M. N.; Verhoeven, J. W. *Chem. Phys. Lett.* **1994**, *230*, 536.
(20) Ghiggino, K. P.; Paddon-Row, M. N.; Craig, D. C. *J. Org. Chem.* **1997**, *62*, 3281.
(21) Zimmerman, H. E.; Goldman, T. D.; Hirzel, T. K.; Schmidt, S. P. *J. Org. Chem.* **1980**, *45*, 3933.
(22) Vögtle, F.; Frank, M.; Nieger, M.; Belser, P.; von Zelewsky, A.; Balzani, V.; Barigelletti, F.; De Cola, L.; Flamigni, L. *Angew. Chem., Int. Ed. Engl.* **1993**, *32*, 1643.
(23) Wang, Z.; Ren, Y.; Zhu, H.; Weininger, S. J.; McGimpsey, W. G. *J. Am. Chem. Soc.* **1995**, *117*, 7, 4367.
(24) Kumar, K.; Lin, Z.; Zimmt, M. B. *J. Am. Chem. Soc.* **1996**, *118*, 243.
(25) Sen, A.; Krishnan, V. *Chem. Phys. Lett.* **1998**, *294*, 499.
(26) Vollmer, M. S.; Effenberger, F.; Stümpfig, T.; Hartschuh, A.; Port, H.; Wolf, H. C. *J. Org. Chem.* **1998**, *63*, 5080.
(27) Hisada, K.; Tsuchida, A.; Ito, S.; Yamamoto, M. *J. Phys. Chem. B* **1998**, *102*, 2640.
(28) Bravo, J.; Mendicuti, F.; Saiz, E.; Mattice, W. L. *J. Fluoresc.* **1996**, *6*, 41.
(29) Bravo, J.; Mendicuti, F.; Saiz, E.; Mattice, W. L. *Macromol. Chem. Phys.* **1994**, *195*, 3411.
(30) Tran, J.; Olmsted, J., III. *J. Photochem. Photobiol. A: Chem.* **1993**, *71*, 45.
(31) Tian, H.-J.; Zhou, Q.-F.; Shen, S.-Y.: Xu, H.-J. *J. Photochem. Photobiol. A: Chem.* **1993**, *72*, 163.
(32) Katayama, H.; Ito, S.; Yamamoto, M. *J. Phys. Chem.* **1992**, *96*, 10115.
(33) Kaschke, M.; Ernsting, N. P.; Valeur, B.; Bourson, J. *J. Phys. Chem.* **1990**, *94*, 5757.
(34) Hassoon, S.; Lustig, H.; Rubin, M. B.; Speiser, S. *J. Phys. Chem.* **1984**, *88*, 6367.
(35) Speiser, S.; Hassoon, S.; Rubin, M. B. *J. Chem. Phys.* **1986**, *90*, 5085.
(36) Levy, S.-T.; Speiser, S. *J. Chem. Phys.* **1991**, *96*, 3587.
(37) Wagner, R. W.; Lindsey, J. S. *J. Am. Chem. Soc.* **1994**, *116*, 9759.

(38) For example: Seth, J.; Palaniappan, V.; Wagner, R. W.; Johnson, T. E.; Lindsey, J. S.; Bocian, D. F. *J. Am. Chem. Soc.* **1996**, *118*, 11194. See also preceding paper in that issue.

(39) Gundermann, K.-D.; Romahn, E.; Zander, M. *Z. Naturforsch.* **1992**, *47A*, 877.

(40) Castellan, A.; Kessab, L.; Grelier, S.; Nourmamode, A.; Cotrait, M.; Marsau, P. *J. Chem. Soc., Perkin Trans. 2* **1993**, 931.

(41) Arrhenius, T. S.; Blanchard-Desce, M.; Dvolaitzky, M.; Lehn, J.-M.; Malthete, J. *Proc. Natl. Acad. Sci. U.S.A.* **1986**, *83*, 5355.

(42) Lehn, J.-M. *Angew. Chem., Int. Ed. Engl.* **1988**, *27*, 89.

(43) Aviram, A. *J. Am. Chem. Soc.* **1988**, *110*, 5687.

(44) Tour, J. M.; Wu, R.; Schumm, J. S. *J. Am. Chem. Soc.* **1991**, *113*, 7064.

(45) Pearson, D. L.; Schumm, J. S.; Tour, J. M. *Macromolecules* **1994**, *27*, 2348.

(46) McGimpsey, W. G.; Samaniego, W. N.; Lie, L.; Wang, F. *J. Phys. Chem. A* **1998**, *102*, 8679.

(47) Smith, G. A.; McGimpsey, W. G. *J. Phys. Chem* **1994**, *98*, 2923.

(48) Murov, S. L.; Carmichael, I.; Hug, G. L. *Handbook of Photochemistry*; 1992; Marcel Dekker: New York.

(49) Gessner, F.; Scaiano, J. C. *J. Am. Chem. Soc.* **1985**, *107*, 7206.

(50) Carmichael, I.; Hug, G. L. *J. Phys. Chem. Ref. Data* **1986**, *15*, 1.

(51) See, for example Speiser's detailed treatment of these processes in ref 36 and: Speiser, S. *Chem. Rev.* **1996**, *96*, 1953. See also, for example: refs 22, 25, 29, 32, 33 and: Beecham, J. M.; Haas, E. *Biophys. J.* **1989**, *55*, 1225.

(52) The modeling results given in the text are for the 2-substituted phenanthrene isomer. The interchromophore separations and rotational barriers obtained for the 3-isomer were qualitatively similar.